Published in final edited form as:
Cell. 2013 June 20; 153(7): 1494–1509. doi:10.1016/j.cell.2013.05.026.

PI(4,5)P_2 DEPENDENT AND Ca^{2+}-REGULATED ER-PLASMA MEMBRANE INTERACTIONS MEDIATED BY THE EXTENDED-SYNAPTOTAGMINS

Francesca Giordano[1,3,4,*], **Yasunori Saheki**[1,3,4,*], **Olof Idevall-Hagren**[1,3,4], **Sara Colombo**[5], **Michelle Pirruccello**[1,3,4], **Ira Milosevic**[1,3,4], **Elena O. Gracheva**[2,3], **Sviatoslav N. Bagriantsev**[2], **Nica Borgese**[5,6], and **Pietro De Camilli**[1,3,4,#]

[1]Department of Cell Biology, Yale School of Medicine, New Haven CT, 06510

[2]Department of Physiology, Yale School of Medicine, New Haven CT, 06510

[3]Program in Cellular Neuroscience, Neurodegeneration and Repair, Yale School of Medicine, New Haven CT, 06510

[4]Howard Hughes Medical Institute, Yale School of Medicine, New Haven CT, 06510

[5]CNR Institute of Neuroscience and BIOMETRA Department, Università degli Studi di Milano, 20129, Milan, Italy

[6]Department of Health Science, University “Magna Graecia” of Catanzaro, 88100, Catanzaro, Italy

SUMMARY

Most available information on ER-plasma membrane (PM) contacts in cells of higher eukaryotes concerns proteins implicated in the regulation of Ca^{2+} entry. However, growing evidence suggests that such contacts play more general roles in cell physiology, pointing to the existence of additionally ubiquitously expressed ER-PM tethers. Here we show that the three Extended-Synaptotagmins (E-Syts) are ER proteins that participate in such tethering function via C2 domain-dependent interactions with the PM that require PI(4,5)P_2 in the case of E-Syt2 and E-Syt3 and also elevation of cytosolic Ca^{2+} in the case of E-Syt1. As they form heteromeric complexes, the E-Syts confer cytosolic Ca^{2+} regulation to ER-PM contact formation. E-Syts-dependent contacts, however, are not required for store-operated Ca^{2+} entry. Thus, the ER-PM tethering function of the E-Syts (tricalbins in yeast), mediate the formation of ER-PM contacts sites which are functionally distinct from those mediated by STIM1 and Orai1.

INTRODUCTION

The endoplasmic reticulum (ER) forms a complex network that extends throughout the cell and plays a multiplicity of functions, including protein synthesis, lipid metabolism and Ca^{2+} storage for intracellular signaling. While membranes of the ER are functionally connected to all membranes of the secretory and endocytic pathways via vesicular transport, they only

[#]To whom correspondence should be addressed: pietro.decamilli@yale.edu.
[*]These authors contributed equally to this work

fuse with each other and with vesicles involved in retrograde transport from the Golgi complex. However, there is growing evidence that close appositions between the ER and the membranes of virtually all other membranous organelles play major roles in cell physiology. These sites are thought to be involved in exchanges of molecules such as lipids, in the function of ER-localized enzymes that act “in trans” on the apposed membrane and in the control of Ca^{2+} homeostasis (Elbaz and Schuldiner, 2011; Friedman and Voeltz, 2011; Holthuis and Levine, 2005; Stefan et al., 2011; Stefan et al., 2013; Toulmay and Prinz, 2011).

In cells of higher eukaryotes, ER-PM contact sites were first described by electron microscopy in the 1950's in muscle (Porter and Palade, 1957), where they are extremely abundant. They were subsequently observed also in neurons (Rosenbluth, 1962). More recently, it has become clear that they represent a general feature of all eukaryotic cells, although, due to their small size in most cells, they are frequently overlooked in electron micrographs (Friedman and Voeltz, 2011).

A well-established function of ER-PM junctions in metazoan cells is control of Ca^{2+} dynamics. In muscle, they are responsible for depolarization-contraction coupling (Endo, 2009), as they are sites where the juxtaposition of voltage-dependent Ca^{2+} channels in the PM and ryanodine receptors in the ER membrane couple Ca^{2+} entry from the extracellular space to Ca^{2+} release from the ER (Block et al., 1988; Franzini-Armstrong and Jorgensen, 1994; Takeshima et al., 2000). ER-PM contact sites are also responsible for store-operated Ca^{2+} entry (SOCE). Oligomerization of the ER protein STIM1 in response to lowered Ca^{2+} levels in the ER lumen triggers its interaction with, and activation of, the PM Ca^{2+} channel Orai1, leading to Ca^{2+} influx to restore normal Ca^{2+} levels in the ER (Feske et al., 2006; Lewis, 2007; Liou et al., 2005; Orci et al., 2009; Zhang et al., 2005). While depletion of intracellular Ca^{2+} stores enhances areas of apposition between the PM and the ER, focal ER-PM contact sites exist before STIM1 recruitment (Orci et al., 2009; Shen et al., 2011). This is consistent with the presence of ER-localized enzymes expected to act “in trans” on PM substrates (Anderie et al., 2007; Stefan et al., 2011) and of ER proteins (VAP-A and VAP-B) that bind PM interacting proteins (Levine and Loewen, 2006; Schulz et al., 2009). However, neither these ER enzymes, nor VAP family proteins, are selectively localized at ER-PM contacts, speaking against their specialized role in the generation of such sites.

In yeast, where some of the metabolic functions requiring direct ER to PM apposition have been characterized (Holthuis and Levine, 2005; Stefan et al., 2011), the bulk of the ER (more than 50%) has a cortical localization (West et al., 2011). Thus, studies of proteins that mediate cortical ER formation in yeast may help elucidate the most fundamental properties of ER-PM contacts. Recently, three yeast ER proteins, the tricalbins (Tcb1p, Tcb2p and Tcb3p), were shown to be selectively concentrated in the cortical ER and to play a key role in ER-PM tethering (Manford et al., 2012; Toulmay and Prinz, 2012). Tricalbins are ER integral membrane proteins with a cytosolic SMP domain followed by multiple C2 domains (Creutz et al., 2004; Lee and Hong, 2006). SMP domains, which are lipid-binding modules, are proposed to have specialized function at membrane contact sites, possibly in lipid exchange between the two membranes (Kopec et al., 2010; Toulmay and Prinz, 2012). C2 domains are generally acidic phospholipid-binding modules, and thus have the potential to bind the PM in trans (Rizo and Sudhof, 1998). Mammalian cells express three proteins that share sequence and domain similarity to the tricalbins, the extended-synaptotagmins (E-Syt1, E-Syt2 and E-Syt-3) (Lee and Hong, 2006; Min et al., 2007). Based on the expression of epitope-tagged constructs in mammalian cells, E-Syt1 was reported to localize in an undetermined intracellular compartment while E-Syt2 and E-Syt3 were reported to localize to the PM (Min et al., 2007).

We have now found that all three E-Syts are ER-anchored proteins. They form homo- and heteromeric complexes that mediate contacts with the PM. Such contacts are critically dependent on the presence of $PI(4,5)P_2$ in this membrane and are additionally regulated by cytosolic Ca^{2+}, via the Ca^{2+}-sensing property of E-Syt1. As they are not required for SOCE, they are functionally distinct from the STIM1-induced contacts.

RESULTS

E-Syts localize to ER and their overexpression induces cortical ER

The subcellular targeting of each E-Syt protein was analyzed by transfecting cells with tagged constructs whose expression was confirmed by western blotting (none of the available antibodies produced a specific immunocytochemical signal). To rule out artifacts due to tag-induced mistargeting, multiple constructs were used, including E-Syts tagged with EGFP or mCherry at the N- or C-terminus, or with small N- or C-terminal tags (Myc or FLAG) (Figures 1 and S1). In the following text, the position of the tag name relative to the protein name indicates its N- or C-terminal location respectively. All constructs yielded similar results. As previously described using the same approach (expression of tagged constructs) (Min et al., 2007), E-Syt1 had a broad intracellular distribution, while E-Syt2 and E-Syt3 had a predominant PM-like localization, although in some cells we detected a substantial intracellular pool of E-Syt2 (Figures 1B and S1B–S1D, S1H, S1K). E-Syt1 colocalized with the co-transfected ER marker Sec61β fused to mRFP (mRFP-Sec61β) (Shibata et al., 2008), indicating a localization throughout the ER (Figures 1B and S1A, S1G). While E-Syt2 and E-Syt3 had a very different localization from E-Syt1, their expression, which resulted in overexpression relative to the endogenous proteins (Figure S1E), shifted a pool of mRFP-Sec61β to the cell periphery where it colocalized with E-Syt2 and E-Syt3 (insets of Figure 1B). When present, the non-cortical pool of E-Syt2 also colocalized with Sec61β (Figures S1B and S1H). A cortical shift of a pool of mRFP-Sec61β was also observed in cells overexpressing untagged E-Syt2 and E-Syt3, further excluding tag-induced artifacts (Figure S1F).

To determine whether the Sec61β signal overlapping with E-Syt2 and E-Syt3 at the cell periphery represented cortical ER, HeLa cells overexpressing E-Syt2 or E-Syt3 with or without a C-terminal EGFP tag were examined by electron microscopy. Some cells used for this analysis were additionally transfected with horseradish peroxidase (HRP) tagged with an ER retention motif (ssHRP-KDEL) (Schikorski et al., 2007), so that the ER could be identified via an electron dense (dark) HRP reaction product. In control cells, contacts between the ER-PM contacts were generally few in individual sections and small in size (Figures 1C and 7A). However, in cells overexpressing E-Syt2, and even more so in cells overexpressing E-Syt3, a massive presence of ER elements closely apposed to the PM via a ribosome-free surface (average distance of 10±3 nm) was observed (arrows in Figures 1D–H).

E-Syt2 and E-Syt3 localize at sites of apposition between the ER and the PM

The ability of E-Syt2 and E-Syt3 to induce cortical ER suggests that they directly participate in bridging the two membranes. If so, they should be localized at the interface of the two membranes. To test this hypothesis, anti EGFP-immunogold EM (10 nm gold) was performed on ultrathin frozen sections of E-Syt-EGFP expressing HeLa cells. Consistent with fluorescence imaging, E-Syt2-EGFP (Figure 1I) and E-Syt3-EGFP (Figure 1J) were highly concentrated at the expanded areas of apposition between the PM and the ER, which were identified by co-immunolabeling (5 nm gold) for endogenous protein disulfide isomerase (PDI), a resident luminal protein of the ER. No immunogold was observed on regions of the PM not in contact with the ER (Figures 1I and 1J). In agreement with

fluorescence imaging, E-Syt1-EGFP was broadly detected on ER elements throughout the cell (arrows, Figure 5C). Notably however, at the few and small ER-PM contacts visible in these cells, anti E-Syt1-EGFP immunogold was frequently observed (arrowhead in Figure 5C).

Subcellular targeting of the E-Syts and synaptotagmin 1 (Syt1) is distinct

A selective localization of the E-Syts in the ER contrasts with the predominant localization of the "bona fide" synaptotagmins in post-Golgi membranes (Sudhof, 2002, 2012). Syt1, the founding member of the synaptotagmin family, is localized primarily on synaptic and neurosecretory vesicles in neuronal cells (Perin et al., 1990) and primarily at the PM in non-neuronal cells due to absence in these cells of a specific adaptor needed for its endocytic recycling ((Diril et al., 2006) and Figures 2A, 2B and 2F). The retention of the E-Syts in the ER was unexpected in view of the overall similarities between the two protein families: a single "predicted" transmembrane region preceded by a short amino acid sequence and followed by a large cytosolic domain comprising C2 domains. Thus we performed a direct comparison, under the same conditions, of the subcellular targeting of the E-Syts and of Syt1.

In HeLa cells Syt1-EGFP produced an uninterrupted decoration of the PM, including its filopodia (Figure 2A). This fluorescent pattern was different from the somewhat discontinuous PM lining of E-Syt2 and E-Syt3 that never extended into the filopodia (compare with Figure 1B). Furthermore, when a small N-terminal Myc-tag was added to Syt1, the tag could be detected at the cell surface in non-fixed non-permeabilized HeLa cells kept at 4°C (Figure 2B). In contrast, no signal of identically N-terminally Myc-tagged E-Syts was detected at the cell surface under these conditions (Figures 2C–2E). Similarly, surface accessibility of Syt1 and non-accessibility of the E-Syts were observed in SH-SY5Y neuroblastoma cells (Figure 2F). In these cells, an additional punctate localization of Syt1 that did not colocalize with the ER marker Sec61β could be observed in the cytoplasm after fixation and Triton X-100 permeabilization, as expected for secretory vesicle localization. In contrast, the localization of the E-Syts, as revealed by anti-Myc antibodies following fixation and permeabilization, was the same as that observed in non-neuronal cells: a localization that globally overlaps with that of the co-transfected Sec61β for E-Syt1 and a cortical localization that only overlaps with a peripheral pool of Sec61β for E-Syt2 and E-Syt3 (Figures 2F).

E-Syts associate with the ER membrane bilayer via a hairpin sequence

An additional difference between the E-Syts and Syt1 was revealed by the characterization of the topology of the E-Syts in the membrane. The E-Syts, like Syt1, were proposed to be integral membrane proteins with the N-terminus localized in the non-cytosolic space and a single transmembrane span originating from a type I signal-anchor sequence (Lee and Hong, 2006; Min et al., 2007; Toulmay and Prinz, 2012). In Syt1, which like the E-Syts lacks a signal sequence, the addition of a folded module (but not of a short epitope) to its N-terminus prevents its translocation across the ER membrane (Kida et al., 2005). Accordingly, addition of an EGFP tag without a signal sequence to the N-terminus of Syt1 disrupts its localization resulting in large aggregates (Figure S1J). In contrast, E-Syts harboring folded modules (EGFP or mCherry) without a signal sequence at their N-terminus, had the same localization and intracellular dynamics as C-terminal tagged E-Syts (Figures S1G–S1I and S1K) raising the possibility that their N-termini may not be translocated across the membrane. As only one potential membrane anchoring sequence is predicted in the E-Syts by hydrophilicity analysis (Figure S2J), the cytosolic location of both the N- and C-termini could be explained by a hairpin structure of this hydrophobic sequence.

Inspection of the putative transmembrane segments of all three E-Syts reveals that their length, 30–31 amino acids (Figure 3A), not only exceeds the length of the transmembrane region of the synaptotagmins (reported as 27 a.a. for synaptotagmin II)(Kida et al., 2005) and of other proteins of post-Golgi membranes, but, more importantly, exceeds that of the transmembrane regions of typical integral membrane proteins of the ER (on average about 20 a.a.) (Higy et al., 2004; Sharpe et al., 2010). This length is compatible with formation of a hairpin that penetrates, but does not cross entirely, the bilayer, as shown for the hydrophobic membrane stretches of several other ER proteins, such as the reticulons (Voeltz et al., 2006). The putative transmembrane domain of the yeast tricalbins has similar characteristics, and is in fact slightly longer, with a charged amino acid in its center consistent with a hairpin spanning the entire bilayer (Figure 3A).

To determine whether the N-termini of the E-Syts are exposed to the cytosol, the PM of cells co-expressing each N-terminally Myc-tagged E-Syt and the luminal ER marker ER-mRFP was selectively permeabilized with low concentrations of digitonin [a treatment that does not permeabilize the ER membrane (Lorenz et al., 2006)] and accessibility of the Myc epitopes was probed with fluorophore-conjugated anti-Myc antibodies without any fixation. While ER-mRFP was retained in the ER lumen as expected (Figures S2E–S2F), strong staining of the Myc epitopes was obtained under this condition (Figures 3B–3D), indicating that the N-termini of all three E-Syts are accessible to the cytosolic surface of the ER.

Consistent with these findings, both the N-, C-terminally and even internally linked fluorescent tags of E-Syts, like the C-terminally linked mCherry-tag of Sec61β (cytosolic mCherry, positive control), were accessible to protease K digestion, with total loss of fluorescence within 1 min upon digitonin treatment of non-fixed cells (Lorenz et al., 2006). In contrast the fluorescence of VAP-A-EGFP (luminal EGFP, negative control) was not affected (Figures S2A–S2I and Supplemental movies 1 and 2)

Finally, the mode of insertion of Syt1 and of an E-Syt was directly assessed by a cell-free translation-translocation assay (Brambillasca et al., 2005). When Myc-Syt1 and Myc-E-Syt3 were translated in the presence of rough microsomes, resistance to alkaline extraction demonstrated that both proteins became tightly integrated in the ER membrane (Figures S2L). This fits with the observation that endogenous E-Syt1, like other integral ER membrane proteins such as calnexin and VAP-A, is resistant to alkaline and high salt extraction (Figure S2M). In the case of Myc-Syt1, an upward mobility shift of the translation product in the cell free assay reflected utilization of an N-glycosylation site in the N-terminal region [abolished by the N-glycosylation inhibitor (NYT)], thus demonstrating its translocation (Figure 3E, first three lanes). As E-Syt3 lacks an N-glycosylation consensus sequence, translocation was assessed by proteinase K protection of metabolically ($^{[35S]}$Methionine) labeled proteins (see cartoon in Figure S2K). Anti-Myc immunoprecipitation followed by autoradiography revealed that a Myc-positive fragment was protected upon exposure of non-permeabilized microsomes to proteinase K in the case of Myc-Syt1 but not in the case of Myc-E-Syt3, although the full-length products were immunoprecipitated with equal efficiency (Figure 3E). These results demonstrate the translocation of the N-terminus of Myc-Syt1 but not Myc-Syt3.

Collectively, these results strongly support the hypothesis that the E-Syts are inserted in the ER through a hairpin sequence (Figure 3F).

Interaction of the C2C domain of E-Syt2 and E-Syt3 with PM PI(4,5)P_2

A tethering function of E-Syt2 and E-Syt3 at the ER predicts that their cytosolically exposed domains bind “in trans” the PM. Their C2C domains could contain such a binding site, as this domain was reported to be required for the peripheral localization (interpreted as a *bona*

fide PM localization) localization of E-Syt2 and E-Syt3 (Min et al., 2007). Accordingly, E-Syt2 and E-Syt3 constructs lacking the C2C domain had a diffuse localization throughout the ER (Figures 4A, 4B and S3B). Conversely, a deletion construct lacking the putative transmembrane region but containing the C2 domains (E-Syt2 C2ABC) (Figure 4I) and even the C2C domain alone (E-Syt2 C2C) (Figure 4B), were recruited to the PM, while a construct that lacks the SMP domain, E-Syt2 SMPΔ, was still recruited to cortical ER (Figure S3A).

C2 domains are phospholipid binding modules, and for many of them the interaction of a surface exposed basic patch with acidic phospholipid bilayers is enhanced by $PI(4,5)P_2$ (Chapman, 2008; Fernandez et al., 2001; Rizo and Sudhof, 1998), a phosphoinositide primarily concentrated in the PM (Di Paolo and De Camilli, 2006). The basic patch, but not the amino acids responsible for Ca^{2+} binding in a subset of C2 domains (Chapman, 2008; Fernandez et al., 2001), is present in the C2C domains of E-Syt2 and E-Syt3 (Figure S4A). Supporting a role of acidic phospholipids in E-Syt2 and E-Syt3 targeting, mutation of the basic residues (K805A, R806A, R807A, R810A, R811A, and K812A) responsible for the basic patch in the C2C domain of E-Syt2 abolished its cortical localization and resulted in a distribution of E-Syt2 throughout the ER (Figure 4B).

To directly test the role of $PI(4,5)P_2$ in E-Syt2 and E-Syt3 recruitment, we rapidly depleted this phosphoinositide in the PM using an optogenetic system recently developed in our lab. The system is based on the blue light-dependent heterodimerization of a cytosolically localized inositol 5-phosphatase domain with a PM targeted module (Idevall-Hagren et al., 2012)(Figure S3C).

COS-7 cells were co-transfected with 1) the two components of the heterodimerization system (CIBN-CAAX and CRY2-5-$ptase_{OCRL}$), 2) a $PI(4,5)P_2$ reporter (iRFP-PH-$PLC_{\delta 1}$ or EFGP-PH-$PLC_{\delta 1}$) and 3) either E-Syt2 or E-Syt3 constructs. Prior to illumination, robust signals for both E-Syt2 and E-Syt3 and the $PI(4,5)P_2$ reporter were detected in the cortical region of the cell by either TIRF or confocal microscopy (arrows, Figure 4C, 4G and 4H and movie S3). Upon blue light illumination, the $PI(4,5)P_2$ reporter dissociated within seconds from the PM, consistent with $PI(4,5)P_2$ dephosphorylation (Figure 4C). This change correlated with a dispersion of E-Syt3 fluorescence from the cell periphery into the typical ER reticular network distributed throughout the cell, including the nuclear envelope (Figure 4C, 4G and movie S3). Similar results were obtained for E-Syt2(Figure 4H and movie S4). The mCherry-tagged C2ABC region of E-Syt2 (Figure 4A) also relocated from the PM to the cytosol upon acute $PI(4,5)P_2$ depletion (Figure 4I). Both the relocation of the $PI(4,5)P_2$ reporter and of the E-Syts were reversible within minutes upon interruption of blue light illumination likely due to $PI(4,5)P_2$ resynthesis (Idevall-Hagren et al., 2012). None of the effects described were elicited by a catalytically inactive mutant of the 5-phosphatase(Figure 4J).

Double immunogold labeling for E-Syt3-EGFP and for the luminal ER marker PDI on ultrathin cryosections of cells fixed during exposure to blue light confirmed the massive re-distribution of E-Syt3 (arrows, Figure 4D) from the cell periphery to the entire ER network (marked by PDI) (Figures 4D and 4E) and showed that this change was accompanied by 80% loss of cortical ER (Figure 4F). Additionally, TIRF microscopy imaging of E-Syt2-EGFP and a luminal ER-marker (ER-mRFP) showed loss of both proteins from the cortical region of the cell during light-induced $PI(4,5)P_2$ depletion (Figure S3D), indicating loss of cortical ER structures.

Ca^{2+} dependent recruitment of E-Syt1 to the PM

Several C2 domains bind $PI(4,5)P_2$ in a Ca^{2+}-dependent way. Inspection of the C2 domains of the E-Syts revealed that amino acids required to confer both Ca^{2+} and acidic phospholipid binding to Syt1 (Fernandez et al., 2001) are most conserved in the C2C domain of E-Syt1 (Figure S4A). Thus we asked whether recruitment of E-Syt1 to the cell cortex depends on elevation of cytosolic Ca^{2+}. Addition to cells expressing EGFP-E-Syt1 of 2 μM thapsigargin (TG), a drug that increases cytosolic Ca^{2+} by blocking its reuptake into the ER and by activating SOCE without major effects on PM $PI(4,5)P_2$ (Liou et al., 2005), resulted in the translocation of E-Syt1 to the cell cortex, as seen by both fluorescence microscopy (TIRF and confocal) and immuno-EM (Figures 5A–5D and S4B and movie S5).

As this experiment did not exclude the possibility that E-Syt1 translocation requires ER Ca^{2+} depletion rather than cytosolic Ca^{2+} increase, the role of rapid cytosolic Ca^{2+} elevation was directly tested using Ca^{2+} uncaging. As shown by confocal microscopy, photolysis of caged Ca^{2+} in HeLa cells expressing mCherry-E-Syt1 induced a transient accumulation of this protein at the cell cortex, which was accompanied by the recruitment of the fluorescent ER luminal marker ER-oxGFP (see extended experimental procedures), reflecting formation of cortical ER (Figures 5F [left panel] and S4C and movie S6). A lower amplitude increase of this signal was also observed in cells not expressing exogenous E-Syt1 (Figure S4C), indicating a physiological role of cytosolic Ca^{2+} in controlling dynamic ER-PM contacts and suggesting a potential role of endogenous E-Syt1 in these actions.

The translocation of E-Syt1, and correspondingly of the ER, to the PM in response to both thapsigargin and to Ca^{2+} uncaging was suppressed in cells where PM $PI(4,5)P_2$ was depleted by the optogenetic approach and also abolished by mutations in the C2C domain of E-Syt1 that disrupt its binding to Ca^{2+} (D663A, D675A, D722A, D724A, D726A, D728A, D729A) (Figures 5E–5G). Thus, this redistribution most likely reflects Ca^{2+}-dependent $PI(4,5)P_2$ binding.

An interplay of cytosolic Ca^{2+} elevation and PM $PI(4,5)P_2$ was further demonstrated by another manipulation: stimulation of PLC by the muscarinic agonist oxotremorine M (OxoM) in cells overexpressing the muscarinic acetylcholine receptor. The increase in cytosolic Ca^{2+} produced by OxoM is triggered by IP3, whose generation involves the consumption of $PI(4,5)P_2$. Thus Ca^{2+}-dependent recruitment of E-Syt1 should be rapidly suppressed by the massive loss of $PI(4,5)P_2$ in the PM. Accordingly, an immediate, prominent, but only very transient recruitment of E-Syt1, and of the ER marker ER-oxGFP was produced by OxoM (Figures 5H and 7C).

Reciprocal interactions of E-Syts

Members of the tricalbin/E-Syt family were reported to form dimers and multimers (Creutz et al., 2004; Groer et al., 2008; Jean et al., 2010). If E-Syt1 and E-Syt2/E-Syt3 interact, they may affect each other's localization. Supporting this possibility, when E-Syt1-EGFP was co-expressed with E-Syt2-mCherry or even more with E-Syt3-mCherry, an increase in the fraction of E-Syt1-EGFP located in cortical ER was observed both by fluorescence and by immunogold electron microscopy (Figures 6A–6C). Conversely, co-expression of E-Syt1 and E-Syt2 resulted in a substantial pool of E-Syt2 detectable throughout the ER. In agreement with the occurrence of a pool of E-Syt2 associated with E-Syt1 in non-cortical ER, a small transient increase of E-Syt2-mCherry fluorescence was observed upon OxoM stimulation prior to the decrease due to $PI(4,5)P_2$ depletion, and this peak was abolished in cells when endogenous E-Syt1 expression was reduced by RNAi (see below evidence for efficient RNAi-mediated E-Syt knockdown) (Figures 6D–6F). As expected, the muscarinic receptor antagonist atropine reversed these changes and even induced excess cortical

accumulation of E-Syt2, a finding that was not further investigated. Conversely, in agreement with the presence of a pre-existing E-Syt1 pool at the cell cortex in cells co-expressing E-Syt1 and E-Syt2, the transient peak of mCherry-E-Syt1 signal observed by TIRF microscopy upon OxoM stimulation was lower than in cells where E-Syt1 was expressed alone, and a reduction of fluorescence relative to the pre-stimulation level was observed after this peak, consistent with loss of cortical E-Syt2 upon $PI(4,5)P_2$ depletion (Figures 6G and 6H). Once again, the OxoM antagonist, atropine, reverted these changes to normal levels.

Formation of E-Syt complexes was supported by biochemical experiments. The presence of untagged E-Syts in immunoprecipitates from extracts of cells doubly transfected with EGFP-tagged and Myc-tagged forms of each E-Syt demonstrated homomerization (Figure S5A). Likewise, the presence of untagged E-Syt1 in anti-EGFP immunoprecipitates from cells co-transfected with this protein and with E-Syt2-EGFP or E-Syt3-EGFP, and of untagged E-Syt2 or E-Syt3 in cells co-transfected with these proteins and with E-Syt1-EGFP (arrows, Figures 6I, 6J and S5B) demonstrated that E-Syt2/3 and E-Syt1 heterodimerize or heteromultimerize. Comassie blue-stained SDS-PAGE gel analysis of TAP (Tandem Affinity Purification)-tagged E-Syt2 (EGFP-TEV-3xFLAG-E-Syt2) immunoprecipitates confirmed robust complex formation of E-Syt2 with an endogenous protein identified by mass spectrometry as E-Syt1 (Figure 6K).

E-Syt triple knock-down reduces ER-PM contact sites and their expansion in the response to cytosolic Ca^{2+} elevations

The results reported so far show that the E-Syts can tether the ER to the PM. To test their requirement for ER-PM contacts, their expression was reduced by RNAi in HeLa cells. Robust suppression of all isoforms was confirmed by Real-Time qPCR and by western blotting for E-Syt1 and E-Syt2 (E-Syt3 was undetectable in HeLa cells by western blotting due to low expression levels) (Figures S6A–S6C).

Triple knock-down (TKD) of all E-Syts resulted in significant reduction (~50%) of the ER-oxGFP signal visible by TIRF microscopy (representing close ER-PM appositions) (Figures S6D and S6E) and this phenotype was rescued by co-expression of untagged siRNA-resistant E-Syt1 and E-Syt2 (Figure S6E). At the EM level, ER-PM contacts, visualized by the electron dense reaction product in the ER of cells transfected with ssHRP-KDEL, decorated about 2% of the PM perimeter in control cells, but only about 0.5% in TKD cells (Figures 7A and 7B).

Knock-down of the three E-Syts also impaired the Ca^{2+}-induced increase of ER-PM appositions. In control cells expressing ER-oxGFP and the muscarinic G-protein-coupled receptor, addition of Oxo-M resulted in rapid and transient recruitment of the ER marker to the cell surface, which was seen as the appearance of fluorescent puncta visualized by TIRF microscopy. This recruitment was abolished in TKD cells, and restored upon expression of untagged E-Syt1 and E-Syt2 (Figures 7C–7F). Thus the E-Syts regulate not only the formation of ER-PM contacts but also the expansion of these contacts in a cytosolic Ca^{2+}-regulated way.

E-Syts knockdown does not affect SOCE

Given the critical role of ER-PM contacts in SOCE mediated by STIM1-Orai1 (Cahalan, 2009; Hogan et al., 2010), we asked whether the E-Syts have an impact on this system. In control conditions, STIM1 is broadly distributed throughout the ER, and its clustering upon Ca^{2+} depletion leads to its interaction with Orai1 in the PM, thus generating cortical ER (Wu et al., 2006). This cortical ER has a very narrow lumen (“thin” ER), possibly due to

aggregation of the luminal domain of STIM1, leading to exclusion of other ER proteins (Orci et al., 2009).

In untreated HeLa cells co-expressing mRFP-STIM1 and EGFP-E-Syt1, only weak E-Syt1 and STIM1 fluorescence was detectable in the TIRF field. Addition of TG in the presence of extracellular Ca^{2+} induced a punctate accumulation of both proteins at the cell cortex. The recruitment of EGFP-E-Syt1 due to cytosolic Ca^{2+} elevation occurred with faster kinetics and was transient, while the recruitment of mRFP-STIM1 due to depletion of Ca^{2+} from the ER lumen was slower (most likely reflecting, at least in part, aggregation prior to recruitment) and persistent (Figures 7G and 7H).

TIRF microscopy-based quantitative analysis of mRFP-STIM1 recruitment to the cell periphery upon TG treatment showed a reduction (~50%) (Figure S6F) after RNAi-mediated E-Syt TKD, which could be at least partially explained by a global reduction in the proximity of the ER to the PM in the absence of the E-Syts since a large pool of STIM1 remain localized to the non-cortical ER even after ER Ca^{2+} depletion (Orci et al., 2009; Wu et al., 2006). However, in TKD cells, robust bright spots of colocalized mRFP-STIM1 and Orai1-EGFP still occurred in the TIRF field upon TG-dependent Ca^{2+} store depletion, although the total area occupied by these spots, as well as their number was reduced (Figure S6 G–I). Furthermore, no significant changes in the rise or peak value of SOCE, as detected by Fura-2, was observed in response to TG treatment in TKD cells (Figure 7I), indicating that E-Syts are not rate limiting for this process. Only the clearance of cytosolic Ca^{2+} after the peak appeared to be delayed, a finding that we have not further investigated.

To gain insight into the lack of an impact of E-Syt TKD on SOCE (at least under the conditions tested), the architecture of ER-PM contacts sites after TG treatment was examined by EM. Ultrastructural analysis, including immunogold labeling, of cells expressing HRP-STIM1 (which broadly labels the ER lumen even after a pool of STIM1 has been recruited to ER-PM contact sites) or YFP-STIM1 confirmed a reduction of cortical ER following TG treatment in TKD cells (Figures 7J–L). Importantly, analysis of these samples revealed that this reduction involved predominantly wide ER structures, while `thin" cortical ER, where anti-YFP immunogold was concentrated and luminal ER proteins were excluded (anti PDI immunogold), was less affected (Figure 7J–M). The presence of abundant "thin" ER even in E-Syt TKD cells may explain the persistence of efficient SOCE.

DISCUSSION

Our results demonstrate that all three E-Syts are resident proteins of the ER and that they function as regulated tethers between the ER and the PM. The interaction of the E-Syts with the PM is mediated by their C2 domains and requires PM $PI(4,5)P_2$, providing another example of the different contexts in which C2 domains are used to tether proteins or organelles to the PM (Figure S6J). In the case of E-Syt2 and E-Syt3, strong binding to the PM occurs at resting Ca^{2+} levels. In contrast, E-Syt1 binding to the PM is triggered by elevation of cytosolic Ca^{2+}, thus mediating or contributing to increased ER-PM appositions in response to Ca^{2+} rise. Interestingly, the C2A domain of E-Syt2 was shown to bind phospholipids in a Ca^{2+}-dependent way, but this interaction did not require acidic phospholipids (Min et al., 2007). Perhaps Ca^{2+} regulates the interaction of this domain "in cis" to the ER membrane, which is not enriched in acidic phospholipids. The requirement of $PI(4,5)P_2$ for E-Syts binding does not rule out additional roles of protein binding partners in the PM. $PI(4,5)P_2$ may simply act as a critically required co-receptor, as shown for many other interactions involving phosphoinositides (Di Paolo and De Camilli, 2006). As the E-Syts homo and heteromerize, the different properties of E-Syts present in heteromeric

complexes may regulate and fine-tune their tethering functions and the functions of the tethers.

The other well-documented house-keeping mechanism responsible for regulated ER-PM contact formation, the STIM1-Orai1 system, is also dependent on changes in intracellular Ca^{2+}. However, STIM1-Orai1 contacts form in response to a loss of intraluminal Ca^{2+} in the ER, rather than to an increase in cytosolic Ca^{2+}(Cahalan, 2009; Hogan et al., 2010). As we have shown here, formation of STIM1-Orai1 contacts, corresponding to "thin" cortical ER in EM sections (Orci et al., 2009), also occurs in the absence of the E-Syts, although less prominently. Accordingly, robust SOCE occurs also in the absence of the E-Syts, when the global numbers or ER-PM contacts are decreased. These results indicate that E-Syts and STIM1-Orai1 represent independent ER-PM cross-talk systems.

Since some ER-PM contacts persist even when the expression levels of E-Syts are greatly reduced, other "in trans" interactions between the ER and the PM are expected to occur. This is consistent with studies in yeast, where the STIM1-Orai1 system is not present and where lack of the tricalbins alone resulted in a reduction, but not in a complete loss of cortical ER (Manford et al., 2012).

The localization of the E-Syts in the ER, an organelle that does not fuse with the plasma membrane, indicates that while their overall domain organization is similar to that of the synaptotagmins, their function is fundamentally different. The synaptotagmins are localized in post-Golgi membranes and are implicated in tethering functions leading to exocytic fusion. This difference is further emphasized by the different topology in the membrane of the two protein families: synaptotagmins are conventional type I transmembrane proteins with a single transmembrane span and the N-terminus in the non-cytosolic space (Kida et al., 2005; Matteoli et al., 1992). In contrast, our data show that the bilayer anchoring stretch of the E-Syts forms a hairpin in the ER membrane so that their N-terminus, like the bulk of the protein with the SMP and C2 domains, is in the cytosol. Interestingly, hairpin insertion in the membrane bilayer has been reported for several other ER proteins, including REEP, the reticulons (Voeltz et al., 2006), spastin, and atlastins (Park et al., 2010). The previously reported accessibility of the N-terminus of the E-Syt2 and E-Syt3 to the extracellular space, which had supported their PM localization, was obtained with cells that were fixed prior to immunostaining (Min et al., 2007), a condition that can result in loss of integrity of the PM. However, our conclusions are consistent with other data of the study by Min et al., such as evidence for the importance of the C2C domains of E-Syt2 and E-Syt3 for their cortical targeting (Min et al., 2007). We cannot rule out that a very small pool of E-Syts may end up in the PM, similar to what is the case of the ER protein STIM1 (Hewavitharana et al., 2008).

In spite of these differences, the property of the E-Syts to tether an intracellular membrane to the PM via C2-dependent interactions with acidic phospholipids is reminiscent of the property of Syt1 to tether secretory vesicles to the PM. Even in the case of Syt1, Ca^{2+}-independent and Ca^{2+}-dependent interactions cooperate, with Ca^{2+}-dependent interactions playing a role in Ca^{2+}-triggered secretory vesicle fusion (Chapman, 2008; Sudhof, 2002, 2012). The presence in the E-Syts of an SMP domain, which is predicted to harbor a lipid within a hydrophobic grove (Kopec et al., 2010), and the observation, further supported by this study, that SMP domains are typically found in protein complexes that tether two membranes (Kornmann et al., 2009; Michel and Kornmann, 2012; Toulmay and Prinz, 2012), have suggested a role of the E-Syts/tricalbins in lipid transfer between the ER and the PM. If further studies validate this hypothesis, it will be of interest to determine how this function is regulated by Ca^{2+}.

In conclusion, our study identifies E-Syts/tricalbins as mediators of ER-PM contact sites and reveal mechanistic and dynamic aspects of these contacts. The conservation of the E-Syt/tricalbin family from yeast to mammals (Manford et al., 2012; Toulmay and Prinz, 2012) emphasizes the general importance of ER-PM contact sites in all eukaryotic cells, irrespective of the very different architecture of the ER in yeast and in higher eukaryotes and of the specialized role of a subset of these junctions, such as the ones involved in the control of Ca^{2+} entry, in animal cells. The characterization of the tricalbin/E-Syt protein family represents a starting point for a precise elucidation of the conserved and most fundamental molecular machinery that controls the cross-talk between the ER and the PM, onto which new functions have been superimposed during evolution to higher eukaryotes.

EXPERIMENTAL PROCEDURES

Full details are provided in the Extended Experimental Procedures.

Cell culture, transfection, RNA interference

HeLa, COS-7 and SH-SY5Y cells were cultured in DMEM containing 10% FBS at 37°C and 5% CO_2. Transfection of plasmids and RNAi oligos was carried out with Lipofectamine 2000 and RNAIi MAX (Life Technologies).

Fluorescence microscopy and optogenetics

Spinning Disc Confocal (SDC) and TIRF microscopy were carried out as described in Extended Experimental Procedures. For optogenetic control of PM $PI(4,5)P_2$, cells were transfected with heterodimerization modules that allow PM recruitment of an inositol-5-phosphatase catalytic domain upon blue light (488 nm) illumination as in (Idevall-Hagren et al., 2012).

Ca^{2+} uncaging

COS-7 cells were loaded with 10μM o-nitrophenyl EGTA-AM (Life technologies) in imaging buffer for 30 min at 37°C. Cells were subsequently washed twice and imaged on a SDC microscope. Photolysis of Ca^{2+} was achieved by a 3 s 405-nm light pulse.

Calcium imaging

HeLa cells were loaded with 5μM Fura-2-AM with Pluronic F127 (invitrogen) in Ca^{2+}-containing buffer for 1 hour at room temperature. Cells were then washed twice and incubated with Ca^{2+}-free buffer before imaging. Thapsigargin (2μM) (Life technologies) was added in Ca^{2+}-free buffer, and Ca^{2+}-containing buffer was added back after Ca^{2+} store depletion.

Antibody accessibility assays and Fluorescent Protease Protection (FPP) assay

To detect cell surface epitopes, live HeLa cells or SH-SY5Y cells co-transfected with Myc-Syt1 or Myc-E-Syts and mRFP-Sec61β were cooled to 4°C and incubated at 4°C with anti-Myc antibodies without fixation (non-permeabilized conditions). Cells were then washed and fixed with 4% PFA/PBS and incubated with Alexa Fluor 488-conjugated anti-rabbit secondary antibody. After further washing, cells were examined with a SDC microscope. As a control, standard immunofluorescence of fixed and permeabilized cells was carried out. To detect cytosolically exposed epitopes on the ER membrane, live HeLa cells expressing Myc-tagged proteins were washed with KHM buffer, followed by KHM buffer containing 20μM digitonin together with anti-Myc Alexa Fluor 488-conjugated antibody. Cells were incubated at RT for 5 min, washed with KHM buffer and fixed with 4% PFA/KHM before

imaging with a SDC microscope. FPP assay was carried out as described previously (Lorenz et al., 2006).

Electron Microscopy

Conventional EM, including HRP cytochemistry, and immunogold labeling of ultrathin frozen sections were performed according to standard procedures (Giordano et al., 2009). EM sections were observed under a Philips CM10 microscope equipped with a Morada 2kx2k CCD camera (Olympus).

Biochemical analysis

For immunoprecipitation of GFP-tagged E-Syts, cell lysates were incubated with Chromotek GFP-trap agarose beads (Allele Biotech), and solubilized bead-bound material was processed for SDS-PAGE and immunoblotting. Tandem affinity purification of EGFP-TEV-3xFLAG-E-Syt2 and the cell-free translation/translocation assay are described in Extended Experimental Procedures.

Statistical analysis

Comparisons of data were carried out using Student's t-test.

Supplementary Material

Refer to Web version on PubMed Central for supplementary material.

Acknowledgments

We thank Scott Emr (Cornell University) for his critical input in this work with discussion of unpublished data. We also thank Frank Wilson for outstanding technical support, Heather Czapla, Yumei Wu, Morven Graham, Xinran Liu and Stacy Wilson for help with microscopy experiments, Nicholas Ingolia (Carnegie Institution for Science) for consultation, Thomas Südhof (Stanford University), Richard S. Lewis (Stanford University), Volker Haucke (Leibniz Institute, Berlin), Dr. Erik Snapp (Albert Einstein College of Medicine), Isabelle Derre and Herve Agaisse (Yale University) for the generous gift of reagents, including unpublished reagents. We also acknowledge Yale Center for Cellular and Molecular Imaging and Yale Center for Genomics and Proteomics. This work was supported in part by grants from the NIH (NS36251, DK082700, DK45735, DA018343) and the Simons Foundation to PDC, the Italian Association for Cancer Research (AIRC grant IG9040) to NB and fellowships from the Uehara Memorial Foundation (YS) and the Swedish Research Council (OIH).

REFERENCES

Anderie I, Schulz I, Schmid A. Characterization of the C-terminal ER membrane anchor of PTP1B. Experimental cell research. 2007; 313:3189–3197. [PubMed: 17643420]

Block BA, Imagawa T, Campbell KP, Franzini-Armstrong C. Structural evidence for direct interaction between the molecular components of the transverse tubule/sarcoplasmic reticulum junction in skeletal muscle. The Journal of cell biology. 1988; 107:2587–2600. [PubMed: 2849609]

Brambillasca S, Yabal M, Soffientini P, Stefanovic S, Makarow M, Hegde RS, Borgese N. Transmembrane topogenesis of a tail-anchored protein is modulated by membrane lipid composition. The EMBO journal. 2005; 24:2533–2542. [PubMed: 15973434]

Cahalan MD. STIMulating store-operated Ca(2+) entry. Nature cell biology. 2009; 11:669–677.

Chapman ER. How does synaptotagmin trigger neurotransmitter release? Annual review of biochemistry. 2008; 77:615–641.

Creutz CE, Snyder SL, Schulz TA. Characterization of the yeast tricalbins: membrane-bound multi-C2-domain proteins that form complexes involved in membrane trafficking. Cellular and molecular life sciences : CMLS. 2004; 61:1208–1220. [PubMed: 15141306]

Di Paolo G, De Camilli P. Phosphoinositides in cell regulation and membrane dynamics. Nature. 2006; 443:651–657. [PubMed: 17035995]

Diril MK, Wienisch M, Jung N, Klingauf J, Haucke V. Stonin 2 is an AP-2-dependent endocytic sorting adaptor for synaptotagmin internalization and recycling. Developmental cell. 2006; 10:233–244. [PubMed: 16459302]

Elbaz Y, Schuldiner M. Staying in touch: the molecular era of organelle contact sites. Trends in biochemical sciences. 2011; 36:616–623. [PubMed: 21958688]

Endo M. Calcium-induced calcium release in skeletal muscle. Physiological reviews. 2009; 89:1153–1176. [PubMed: 19789379]

Fernandez I, Arac D, Ubach J, Gerber SH, Shin O, Gao Y, Anderson RG, Sudhof TC, Rizo J. Three-dimensional structure of the synaptotagmin 1 C2B-domain: synaptotagmin 1 as a phospholipid binding machine. Neuron. 2001; 32:1057–1069. [PubMed: 11754837]

Feske S, Gwack Y, Prakriya M, Srikanth S, Puppel SH, Tanasa B, Hogan PG, Lewis RS, Daly M, Rao A. A mutation in Orai1 causes immune deficiency by abrogating CRAC channel function. Nature. 2006; 441:179–185. [PubMed: 16582901]

Franzini-Armstrong C, Jorgensen AO. Structure and development of E-C coupling units in skeletal muscle. Annual review of physiology. 1994; 56:509–534.

Friedman JR, Voeltz GK. The ER in 3D: a multifunctional dynamic membrane network. Trends in cell biology. 2011; 21:709–717. [PubMed: 21900009]

Giordano F, Bonetti C, Surace EM, Marigo V, Raposo G. The ocular albinism type 1 (OA1) G-protein-coupled receptor functions with MART-1 at early stages of melanogenesis to control melanosome identity and composition. Human molecular genetics. 2009; 18:4530–4545. [PubMed: 19717472]

Groer GJ, Haslbeck M, Roessle M, Gessner A. Structural characterization of soluble E-Syt2. FEBS letters. 2008; 582:3941–3947. [PubMed: 18977228]

Hewavitharana T, Deng X, Wang Y, Ritchie MF, Girish GV, Soboloff J, Gill DL. Location and function of STIM1 in the activation of Ca2+ entry signals. The Journal of biological chemistry. 2008; 283:26252–26262. [PubMed: 18635545]

Higy M, Junne T, Spiess M. Topogenesis of membrane proteins at the endoplasmic reticulum. Biochemistry. 2004; 43:12716–12722. [PubMed: 15461443]

Hogan PG, Lewis RS, Rao A. Molecular basis of calcium signaling in lymphocytes: STIM and ORAI. Annual review of immunology. 2010; 28:491–533.

Holthuis JC, Levine TP. Lipid traffic: floppy drives and a superhighway. Nature reviews Molecular cell biology. 2005; 6:209–220.

Idevall-Hagren O, Dickson EJ, Hille B, Toomre DK, De Camilli P. Optogenetic control of phosphoinositide metabolism. Proceedings of the National Academy of Sciences of the United States of America. 2012; 109:E2316–2323. [PubMed: 22847441]

Jean S, Mikryukov A, Tremblay MG, Baril J, Guillou F, Bellenfant S, Moss T. Extended-synaptotagmin-2 mediates FGF receptor endocytosis and ERK activation in vivo. Developmental cell. 2010; 19:426–439. [PubMed: 20833364]

Kida Y, Mihara K, Sakaguchi M. Translocation of a long amino-terminal domain through ER membrane by following signal-anchor sequence. The EMBO journal. 2005; 24:3202–3213. [PubMed: 16107879]

Kopec KO, Alva V, Lupas AN. Homology of SMP domains to the TULIP superfamily of lipid-binding proteins provides a structural basis for lipid exchange between ER and mitochondria. Bioinformatics. 2010; 26:1927–1931. [PubMed: 20554689]

Kornmann B, Currie E, Collins SR, Schuldiner M, Nunnari J, Weissman JS, Walter P. An ER-mitochondria tethering complex revealed by a synthetic biology screen. Science. 2009; 325:477–481. [PubMed: 19556461]

Lee I, Hong W. Diverse membrane-associated proteins contain a novel SMP domain. FASEB journal : official publication of the Federation of American Societies for Experimental Biology. 2006; 20:202–206. [PubMed: 16449791]

Levine T, Loewen C. Inter-organelle membrane contact sites: through a glass, darkly. Current opinion in cell biology. 2006; 18:371–378. [PubMed: 16806880]

Lewis RS. The molecular choreography of a store-operated calcium channel. Nature. 2007; 446:284–287. [PubMed: 17361175]

Liou J, Kim ML, Heo WD, Jones JT, Myers JW, Ferrell JE Jr. Meyer T. STIM is a Ca2+ sensor essential for Ca2+-store-depletion-triggered Ca2+ influx. Current biology : CB. 2005; 15:1235–1241. [PubMed: 16005298]

Lorenz H, Hailey DW, Wunder C, Lippincott-Schwartz J. The fluorescence protease protection (FPP) assay to determine protein localization and membrane topology. Nature protocols. 2006; 1:276–279.

Manford AG, Stefan CJ, Yuan HL, Macgurn JA, Emr SD. ER-to-plasma membrane tethering proteins regulate cell signaling and ER morphology. Developmental cell. 2012; 23:1129–1140. [PubMed: 23237950]

Matteoli M, Takei K, Perin MS, Sudhof TC, De Camilli P. Exo-endocytotic recycling of synaptic vesicles in developing processes of cultured hippocampal neurons. The Journal of cell biology. 1992; 117:849–861. [PubMed: 1577861]

Michel AH, Kornmann B. The ERMES complex and ER-mitochondria connections. Biochemical Society transactions. 2012; 40:445–450. [PubMed: 22435828]

Min SW, Chang WP, Sudhof TC. E-Syts, a family of membranous Ca2+-sensor proteins with multiple C2 domains. Proceedings of the National Academy of Sciences of the United States of America. 2007; 104:3823–3828. [PubMed: 17360437]

Orci L, Ravazzola M, Le Coadic M, Shen WW, Demaurex N, Cosson P. From the Cover: STIM1-induced precortical and cortical subdomains of the endoplasmic reticulum. Proceedings of the National Academy of Sciences of the United States of America. 2009; 106:19358–19362. [PubMed: 19906989]

Park SH, Zhu PP, Parker RL, Blackstone C. Hereditary spastic paraplegia proteins REEP1, spastin, and atlastin-1 coordinate microtubule interactions with the tubular ER network. The Journal of clinical investigation. 2010; 120:1097–1110. [PubMed: 20200447]

Perin MS, Fried VA, Mignery GA, Jahn R, Sudhof TC. Phospholipid binding by a synaptic vesicle protein homologous to the regulatory region of protein kinase C. Nature. 1990; 345:260–263. [PubMed: 2333096]

Porter KR, Palade GE. Studies on the endoplasmic reticulum. III. Its form and distribution in striated muscle cells. The Journal of biophysical and biochemical cytology. 1957; 3:269–300. [PubMed: 13438910]

Rizo J, Sudhof TC. C2-domains, structure and function of a universal Ca2+-binding domain. The Journal of biological chemistry. 1998; 273:15879–15882. [PubMed: 9632630]

Rosenbluth J. Subsurface cisterns and their relationship to the neuronal plasma membrane. The Journal of cell biology. 1962; 13:405–421. [PubMed: 14493991]

Schikorski T, Young SM Jr. Hu Y. Horseradish peroxidase cDNA as a marker for electron microscopy in neurons. Journal of neuroscience methods. 2007; 165:210–215. [PubMed: 17631969]

Schulz TA, Choi MG, Raychaudhuri S, Mears JA, Ghirlando R, Hinshaw JE, Prinz WA. Lipid-regulated sterol transfer between closely apposed membranes by oxysterol-binding protein homologues. The Journal of cell biology. 2009; 187:889–903. [PubMed: 20008566]

Sharpe HJ, Stevens TJ, Munro S. A comprehensive comparison of transmembrane domains reveals organelle-specific properties. Cell. 2010; 142:158–169. [PubMed: 20603021]

Shen WW, Frieden M, Demaurex N. Remodelling of the endoplasmic reticulum during store-operated calcium entry. Biology of the cell / under the auspices of the European Cell Biology Organization. 2011; 103:365–380. [PubMed: 21736554]

Shibata Y, Voss C, Rist JM, Hu J, Rapoport TA, Prinz WA, Voeltz GK. The reticulon and DP1/Yop1p proteins form immobile oligomers in the tubular endoplasmic reticulum. The Journal of biological chemistry. 2008; 283:18892–18904. [PubMed: 18442980]

Stefan CJ, Manford AG, Baird D, Yamada-Hanff J, Mao Y, Emr SD. Osh proteins regulate phosphoinositide metabolism at ER-plasma membrane contact sites. Cell. 2011; 144:389–401. [PubMed: 21295699]

Stefan, CJ.; Manford, AG.; Emr, SD. Current opinion in cell biology. 2013. ER-PM connections: sites of information transfer and inter-organelle communication.

Sudhof TC. Synaptotagmins: why so many? The Journal of biological chemistry. 2002; 277:7629–7632. [PubMed: 11739399]

Sudhof TC. Calcium control of neurotransmitter release. Cold Spring Harbor perspectives in biology. 2012; 4:a011353. [PubMed: 22068972]

Takeshima H, Komazaki S, Nishi M, Iino M, Kangawa K. Junctophilins: a novel family of junctional membrane complex proteins. Molecular cell. 2000; 6:11–22. [PubMed: 10949023]

Toulmay A, Prinz WA. Lipid transfer and signaling at organelle contact sites: the tip of the iceberg. Current opinion in cell biology. 2011; 23:458–463. [PubMed: 21555211]

Toulmay A, Prinz WA. A conserved membrane-binding domain targets proteins to organelle contact sites. Journal of cell science. 2012; 125:49–58. [PubMed: 22250200]

Voeltz GK, Prinz WA, Shibata Y, Rist JM, Rapoport TA. A class of membrane proteins shaping the tubular endoplasmic reticulum. Cell. 2006; 124:573–586. [PubMed: 16469703]

West M, Zurek N, Hoenger A, Voeltz GK. A 3D analysis of yeast ER structure reveals how ER domains are organized by membrane curvature. The Journal of cell biology. 2011; 193:333–346. [PubMed: 21502358]

Wu MM, Buchanan J, Luik RM, Lewis RS. Ca2+ store depletion causes STIM1 to accumulate in ER regions closely associated with the plasma membrane. The Journal of cell biology. 2006; 174:803–813. [PubMed: 16966422]

Zhang SL, Yu Y, Roos J, Kozak JA, Deerinck TJ, Ellisman MH, Stauderman KA, Cahalan MD. STIM1 is a Ca2+ sensor that activates CRAC channels and migrates from the Ca2+ store to the plasma membrane. Nature. 2005; 437:902–905. [PubMed: 16208375]

HIGHLIGHTS

The three Extended-Synaptotagmins (E-Syts) are ER-localized proteins

E-Syts tether the ER to the PM via C2 domain-PI(4,5)P_2 interactions

E-Syts heteromeric complexes confer Ca^{2+} dependence to ER-PM contact formation

ER-PM contacts mediated by E-Syts are functionally distinct from STIM1-Orai1 contacts

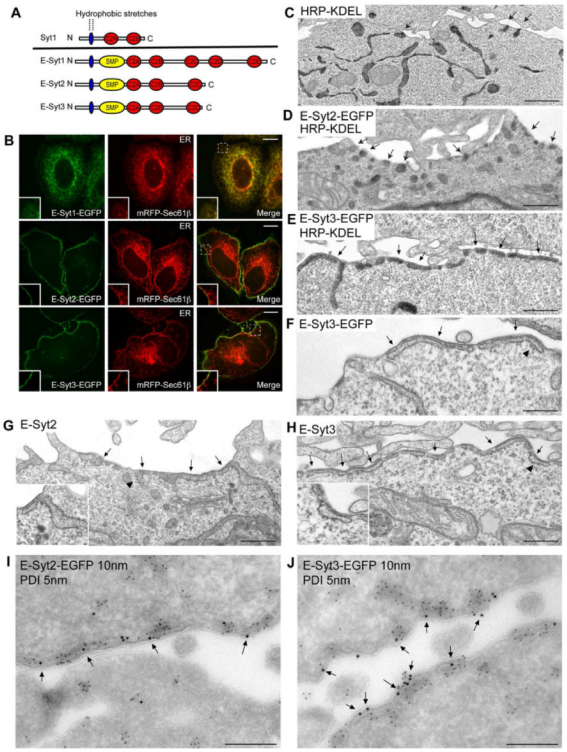

Figure 1. Localization of the E-Syts in the ER and of E-Syt2 and E-Syt3 at ER-PM contact sites

(A) Domain structure of Syt1, and of the E-Syts. (B) Confocal images of HeLa cells expressing E-Syt-EGFP fusions and the ER marker mRFP-Sec61β. Insets show at higher magnification the colocalization throughout the ER for E-Syt1, but only colocalization with the ER marker at the cell periphery for E-Syt2 and E-Syt3. Scale bar, 10 μm. (C–H) Electron micrographs of HeLa cells transfected with the ER luminal marker HRP-KDEL alone (C), or together with E-Syt2-EGFP (D) or E-Syt3-EGFP (E). Cells singly transfected with E-Syt3-EGFP (F), untagged E-Syt2 (G) or untagged E-Syt3 (H). The ER can be identified via an electron dense (dark) HRP reaction product in C–E, and by presence of ribosomes (arrowheads) in F–H. Arrows in C–H indicate cortical ER. Scale bar, 250 nm. (I–J) Electron micrographs of ultrathin cryosections of HeLa cells transfected with E-Syt2-EGFP (I) or E-Syt3-EGFP (J) and double immunogold labeled for EGFP (10 nm gold) to detect E-Syts and for endogenous PDI (5 nm gold) to label the ER lumen. E-Syt2 and E-Syt3 are almost exclusively localized to the cortical ER (arrows). Scale bar, 200nm. See also Figure S1.

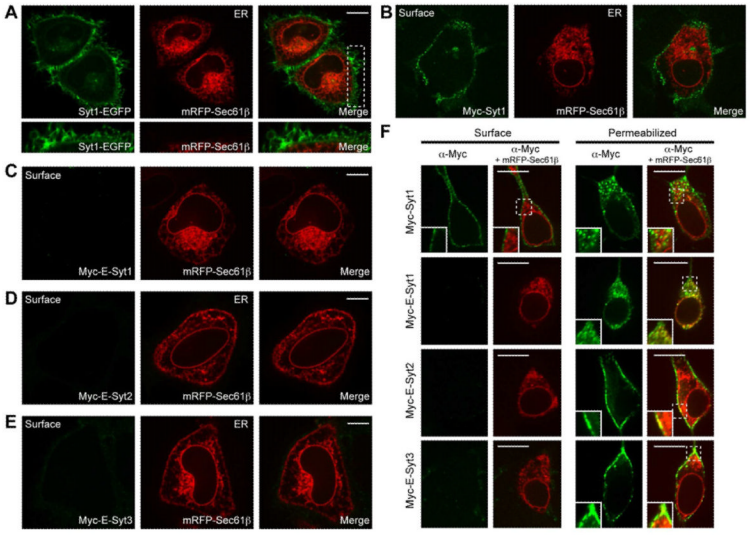

Figure 2. Comparison of the accessibility of the N-termini of Syt1 and of the E-Syts to the extracellular space

(A) Confocal images of live HeLa cells expressing Syt1-EGFP and mRFP-Sec61β showing the predominant PM localization of Syt1 in these cells. Bottom images: high power view of the region outlined by dotted lines in the merge field. (B–E) Fluorescent images of HeLa cells co-expressing mRFP-Sec61β and Myc-Syt1 or Myc-E-Syts as indicated, and incubated with anti-Myc antibodies. The Myc epitope was accessible in the case of Myc-Syt1 but not in the case of Myc-E-Syts. (F) Fluorescent images of SH-SY5Y neuroblastoma cells co-expressing mRFP-Sec61β (red) with either Myc-Syt1 or Myc-E-Syts (green) and incubated with anti-Myc antibodies before fixation (left panels, “surface”) or after fixation and permeabilization (right panel, “permeabilized”). See also Figure S1.

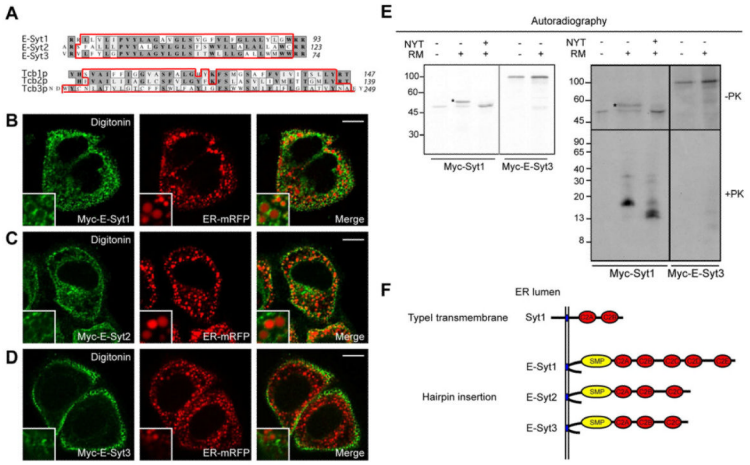

Figure 3. E-Syts are inserted into the ER membranes via hydrophobic hairpin sequences

(A) Alignments of putative transmembrane regions of the three E-Syts (human) and of the three tricalbins. The uncharged residues are contained in the red boxes. Conserved residues and substitutions are shaded in dark and light grey, respectively. The numbers on the right refer to the position of the last residue shown in each sequence. (B–D) Fluorescence images of digitonin-permeabilized (20 μM) HeLa cells co-expressing Myc-E-Syts and ER-mRFP and incubated with Alexa Fluor 488-conjugated anti-Myc antibodies (green) before fixation, showing accessibility of N-terminal Myc epitopes at the surface of ER elements. At the concentration of digitonin used, ER membranes remain unpermeabilized although vesiculated due to cell lysis (see also Figure S2). Scale bar, 10 μm. (E) Cell-free translation-translocation assays showing translocation across microsomal membranes of the N-terminus of Syt1 but not of E-Syt3. (Left panel) Analysis of $^{[35S]}$Met-labeled Myc-Syt1 and Myc-E-Syt3 translated in vitro in the presence or absence of dog pancreas rough microsomes (RM) and N-glycosylation tripeptide inhibitor (NYT), as indicated. An asterisk indicates glycosylated Syt1. (Right panel) Results of protease protection assay. After translation, an aliquot of each fraction was immunoprecipitated with anti-Myc antibodies (upper panel). A ten fold larger aliquot of each sample was subjected to proteinase K (PK) digestion before immunoprecipitation (lower panel). (F) Schematic cartoon showing the topology of Syt1 and of the E-Syts suggested by these experiments. The hydrophobic stretches (about 30 amino acids) previously predicted to cross the membrane are proposed to form hairpins in the ER bilayer. See also Figure S2.

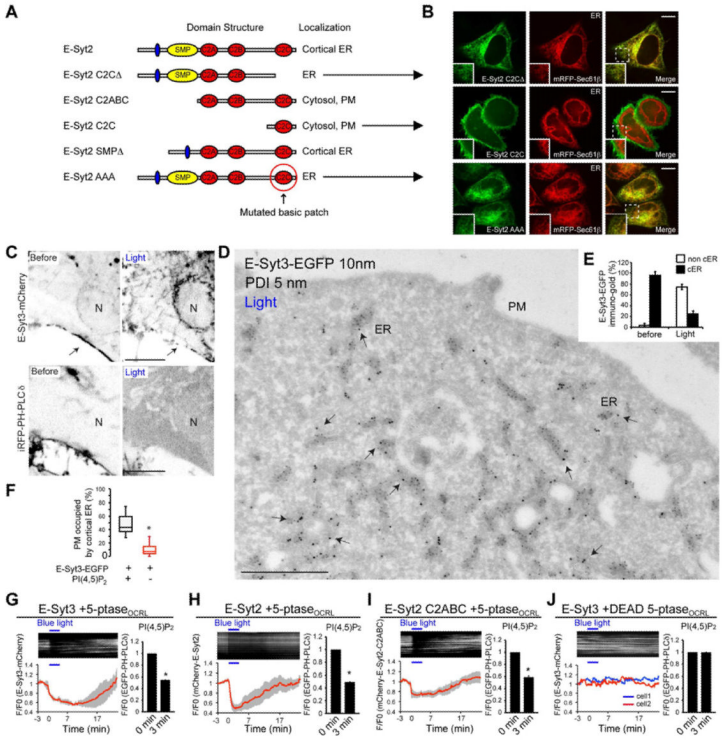

Figure 4. Interaction of the C2C domains of E-Syt2/3 with PM PI(4,5)P_2 is required for the ER-PM tethering function of E-Syt2/3

(A) E-Syt2 constructs examined and their localizations. (B) Confocal images of HeLa cells of constructs lacking the C2C domain or mutated in the basic patch in this domain. The C2C domain alone is targeted to the cell cortex. Scale bar, 10μm. (C) Confocal images of a COS-7 cell expressing E-Syt3-mCherry, the PI(4,5)P_2 reporter iRFP-PH-PLC$_{\delta 1}$, and the two components of blue light-dependent PI(4,5)P_2 depletion system at the end of 10 min blue light illumination (arrow indicates cortical ER). Fluorescence is shown in black. N = nucleus. (see also movie S3). Scale bar, 5μm. (D–F) Immuno-EM micrograph (E-Syt3-EGFP, 10nm gold and endogenous PDI, 5nm gold) of cells processed as above and fixed at the end of the illumination. Quantification of the results is shown in E and F. Note that the redistribution of E-Syt3-EGFP from cell periphery (cortical ER, cER) (compare with Figure 1J) into the non-cortical ER (arrows) is accompanied by loss of cER (mean±SD) (F). * P<0.001. (G – J) Time-course of normalized mCherry fluorescence, as assessed by TIRF microscopy, from COS-7 cells expressing the indicated E-Syt fusion proteins together with EGFP-PH-PLC$_{\delta 1}$ and the two components of blue light-dependent PI(4,5)P_2 depletion system (G – I) or the same two components but with a catalytically inactive phosphatase domain (DEAD 5-ptase$_{OCRL}$) (J). (Top) kymographs of representative cells, and (bottom) average traces (n=5). Data are represented as mean±SEM. The bar graphs on the right show levels of PI(4,5)P_2, as assessed by EGFP-PH-PLC$_{\delta 1}$ fluorescence at time zero and at the end of the 3 min illumination. * P<0.001. See also Figure S3.

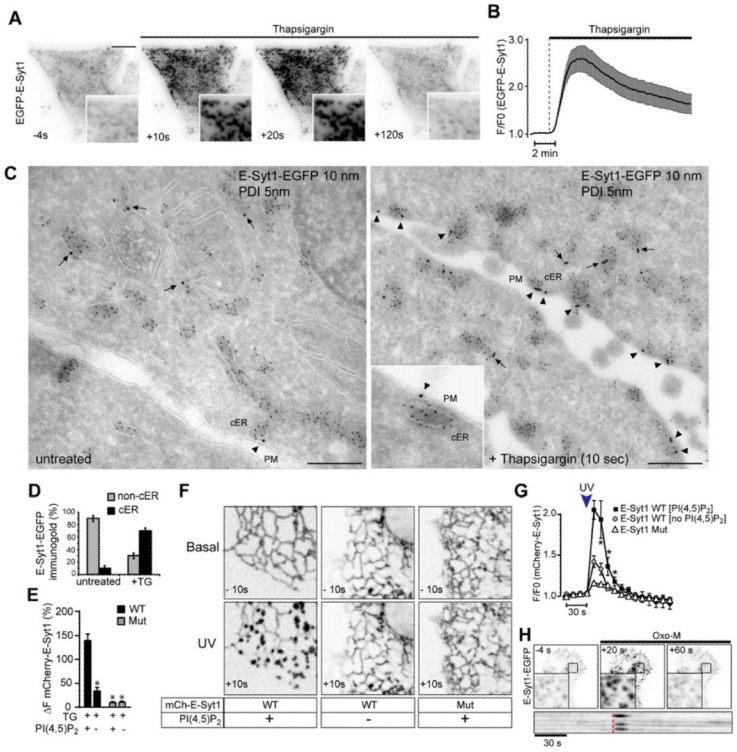

Figure 5. E-Syt1 makes dynamic contacts with the PM in a Ca^{2+}- and $PI(4,5)P_2$-dependent manner

(A) TIRF microscopy images of a HeLa cell expressing EGFP-E-Syt1 before and after stimulation with 2μM thapsigargin (TG) at the indicated times. Scale Bar, 10 μm. (B) Time-course of TG-induced recruitment of EGFP-E-Syt1 to the PM, as shown in A (mean±SEM, n=5). (C) Immuno-EM micrographs of HeLa cells expressing E-Syt1-EGFP, untreated or treated with TG (2 μM, 10 s). E-Syt1-EGFP (10nm gold) and endogenous PDI (5nm gold). Arrows indicate E-Syt1-positive non-cortical ER and arrowheads indicate E-Syt1-positive cortical ER (magnified in the inset). Scale bar, 200 nm. Quantification of the results is shown in D. (means±SD). (E) Quantification of the response of wild-type (WT) or Ca^{2+}-binding deficient (Mut) mCherry-E-Syt1 to TG (2 μM, peak response) in HeLa cells, as assessed by TIRF microscopy, with or without optogenetic depletion of PM $PI(4,5)P_2$ (mean ±SEM, n=3 for each, * $P<0.001$ for comparison to WT [TG]). (F) Confocal images of the ventral region of COS-7 cells expressing WT or Mut mCherry-E-Syt1 before and 10 s after UV photolysis of caged Ca^{2+} with or without optogenetic depletion of PM $PI(4,5)P_2$. Hot spots of fluorescence represent focal accumulation of E-Syt1 at the PM. (G) Time-course of results shown in F (mean±SEM, n=7–15, * $P<0.01$ compared to no $PI[4,5]P_2$). (H) TIRF microscopy images of a HeLa cell expressing E-Syt1-EGFP and the M1 muscarinic receptor (M1R) before and after stimulation with 10 μM oxotremorine-M (Oxo-M). (Bottom) Kymograph of EGFP fluorescence of a representative cell. Fluorescence in A, F and H is shown in black. See also Figure S4.

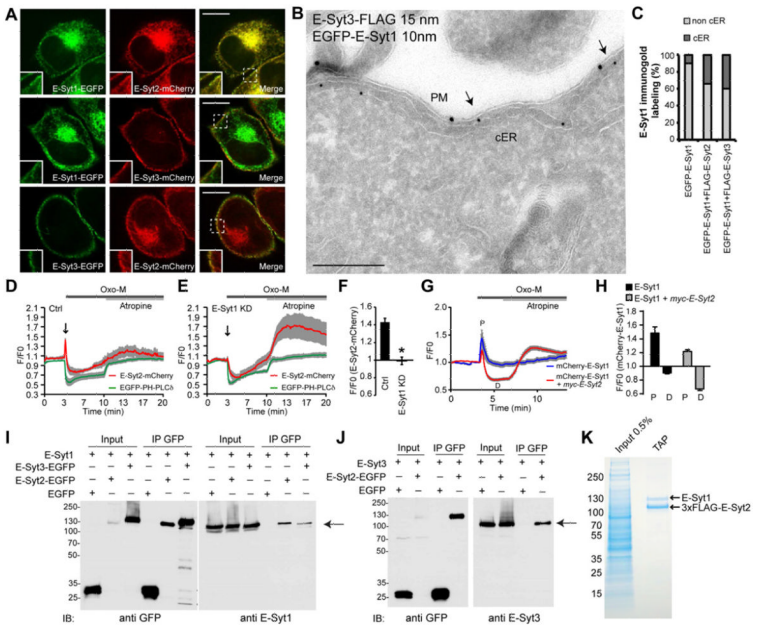

Figure 6. Heteromerization of the E-Syts

(A) Confocal images of HeLa cells co-expressing pairs of EGFP and mCherry E-Syts as indicated. Scale bar, 10 μm. Insets show at higher magnification of the areas framed by a dotted line. (B) Immuno-EM micrograph of HeLa cells co-expressing E-Syt3-FLAG (15nm gold) and EGFP-E-Syt1 (10nm gold and arrows). Scale bar, 200nm. (C) Quantification of immunogold labeling for E-Syt1 on the non-cortical portion of the ER (non-cER) and at ER-PM contact sites (cER) of cells expressing EGFP-E-Syt1 alone or together with 3xFLAG-E-Syt2 or E-Syt3-MycFLAG. Data are represented as mean. (D – E) Time-course of normalized mCherry and EGFP fluorescence, as assessed by TIRF microscopy, from HeLa cells expressing E-Syt2-mCherry and EGFP-PH-PLC$_{\delta 1}$ together with M1R. Cells were treated with either control siRNA (D) or siRNA specific for E-Syt1 (E) and stimulated with Oxo-M (10 μM), followed by addition of atropine (50 μM), as indicated (mean±SEM). (F) Quantification M1 muscarinic receptor of fluorescence corresponding to the peak of E-Syt2 recruitment [arrows in the traces of (D) and (E)] (mean± SEM; * P<0.001). (G – H) Time-course of normalized mCherry fluorescence (TIRF) from HeLa cells expressing mCherry-E-Syt1 alone or together with Myc-E-Syt2. (H) Quantification of fluorescence corresponding to Peak (P) and Drop (D) in the traces of (G) (mean± SEM). (I – J) Extracts of HeLa cells transfected with the constructs indicated were subjected to anti-GFP immunoprecipitation (IP) and then processed for SDS-PAGE and immunoblotting (IB) with anti-GFP, anti-E-Syt1 (I) or anti-E-Syt3 (J) antibodies. Arrows indicate the co-immunoprecipitated bands. Inputs are 2.5% of the total cell lysates. (K) Lysates of HeLa cells expressing EGFP-TEV-3xFLAG-E-Syt2 were tandem affinity purified (TAP) using anti-GFP and anti-FLAG antibodies. Colloidal blue staining of gels of the starting extract (0.5%) and of the affinity-purified material is shown. See also Figure S5.

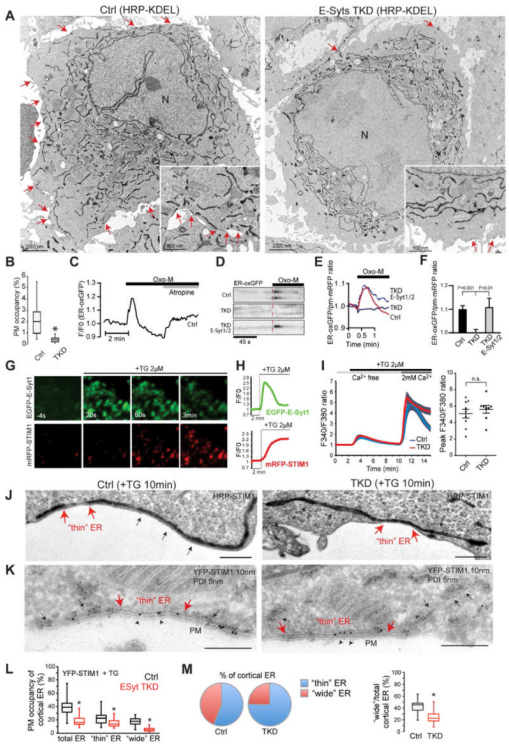

Figure 7. Knockdown of the E-Syts decreases the number of ER-PM contacts but does not impair SOCE

(A) EM micrographs of HRP-KDEL-expressing HeLa cells treated with control siRNA (Ctrl) or siRNAs against the three E-Syts (TKD). Red arrows indicate ER-PM contact sites. N = nucleus. (B) The percentage of PM length engaged in contacts is shown as box and whisker plot (* P<0.001). (C) Time-course of the normalized GFP signal, as assessed by TIRF microscopy, from a HeLa cell expressing a luminal ER marker (ER-oxGFP) and M1R. Oxo-M (10 μM) stimulation and atropine (50 μM) addition are indicated. (D – F) Dynamics of the cortical ER, as visualized by ER-oxGFP fluorescence in the TIRF field, in response to Oxo-M, in control or TKD cells co-expressing the PM marker pm-mRFP and M1R. For rescue, TKD cells were transfected with RNAi-resistant E-Syt1 and E-Syt2. Representative kymographs of the GFP fluorescence (black) and time-course of the normalized ER-oxGFP/pm-mRFP ratios are shown in (D) and (E), respectively. (F) Quantification of fluorescence corresponding to the peaks in E (n=3–10 for each condition). (G) TIRF microscopy images of HeLa cells co-expressing EGFP-E-Syt1 and mRFP-STIM1 before and after the addition of TG (2μM). (H) Time-course of the recruitment of EGFP-E-Syt1 (top) and mRFP-STIM1 (bottom) to the PM. (I) Fura-2 Ca^{2+}-recordings of control and TKD cells. (Left) Time-course of the normalized F340/F380 ratios of cells exposed to TG (2μM) in Ca^{2+}-free medium, followed by Ca^{2+} add-back. The first response corresponds to Ca^{2+} leak from the ER, while the second response corresponds to Ca^{2+} entry from the extracellular medium (SOCE). (Right) SOCE peak values (mean± SEM, n=9 (Ctrl) and n=8 (TKD), n.s.; not significant). (J) EM micrographs of control and TKD cells expressing HRP-STIM1 (dark staining) show cortical ER (cER) upon treatment with TG (2μM). Red arrows delimitate cER with a “thin” lumen. Black arrow indicate “wide” lumen. (K) Immuno-EM micrographs of TG (2 μM) treated control and TKD cells transfected with YFP-STIM1 (anti-GFP, 10nm gold) (arrowheads). Note the exclusion of PDI (5 nm gold) (black arrows) from the “thin” ER (delimited by red arrows) that is preserved in TKD cells. Scale bar, 250 nm. (L) The percentages of PM length in EM sections which is lined by the cortical ER (total), and by

the “thin” and “wide” portions of such ER are shown as Box and whisker plot (* P<0.001). (M) (Left) Pie graphs showing the percentages of the “thin” and the “wide” lumen cER. (Right) Box and whisker plot showing that the relative proportion of the “wide” lumen cER is preferentially decreased in TKD cells (* P<0.001).